RSC Advances

ROYAL SOCIETY OF CHEMISTRY

www.rsc.org/advances

Diffusion Mechanism of Platinum Nanoclusters on Well-Aligned Carbon Nanotubes

Cong Feng[a], Junwei Wang[a], Yumin Cheng[b], Pengfei He[c], and K. M. Liew[d,e,*]

[a] College of Materials Science and Engineering, Key Laboratory for Advanced Civil Engineering Materials (Ministry of Education), Tongji University, Shanghai 201804, China

[b] Shanghai Institute of Applied Mathematics and Mechanics, Shanghai University, Shanghai 200072, China

[c] School of Aerospace Engineering and Applied Mechanics, Tongji University, Shanghai 200092, China

[d] Department of Architecture and Civil Engineering, City University of Hong Kong, Kowloon, Hong Kong Special Administrative Region

[e] City University of Hong Kong Shenzhen Research Institute Building, Shenzhen Hi-Tech Industrial Park, Nanshan District, Shenzhen, China

Carbon supported platinum (Pt/C) remains among the preferred catalyst materials for use in proton exchange membrane fuel cells; however, its durability must be improved. In this work, we considered well-aligned carbon nanotubes (WACNTs) as a carbon support material and investigated the diffusion mechanism of Pt nanoparticles by using molecular dynamic (MD) simulations, including calculation of the binding energy, aggregation probability, and the diffusion coefficient. Moreover, the use of graphene as support material is also examined. The trenches in well-aligned carbon nanotubes were found to not only increase the binding energy between the Pt particles and the substrates but also decrease the aggregation probability of Pt particles comparing with the graphene substrates. Furthermore, we estimated the Pt mass per substrate area (Pt loading) when there is no occurrence or a reduced occurrence of Pt agglomeration: a value of 0.167 $\mu g/cm^2$ for WACNTs (24, 24), and a Pt particle diameter of 2.4 nm are suggested.

1. Introduction

Proton exchange membrane (PEM) fuel cells are the most popular type of fuel cells, due to their fast low-temperature start-up, environmentally clean operation, and high energy conversion efficiency and power density. However, the lifetime of PEM fuel cells used for transportation applications have limited their commercialisation at the current stage, especially the poor durability of the catalyst.[1-3] Currently, carbon structures are predominantly used as the catalyst support due to their unique structures and high electrical conductivity.[4] In particular carbon black has been extensively

---

Corresponding author (K.M Liew). Tel: +852 3442 6581; E-mail: kmliew@cityu.edu.hk

exploited by commercial companies. In addition, carbon nanotubes[5, 6] and graphene[7, 8] are also under consideration as promising catalyst support materials.

However, Pt particles easily suffer from agglomeration and detachment from the carbon support (triggered by carbon corrosion),[9,10] which will result in the loss the electrochemical surface area (ESA) during long-term operation, thereby producing a significant reduction in the fuel cell performance.[11, 12] For example, Bi et al. proposed a physical based Pt/C catalyst model with a simplified bi-modal particle size distribution and used the model to clearly demonstrate the catalyst coarsening via Pt nanoparticle growth.[13] Huang's group observed the detachment and transport of small Pt clusters from the carbon support in their molecular simulations.[14]

It is known that catalytic activity is highly related to the size and dispersion of the Pt particles on the support and to the degree of their interactions.[6,11,15] For example, based on an investigation of the binding energy between one Pt atom and five different graphene surfaces, Groves et al. indicated that the durability of a platinum catalyst can be greatly improved by using the highest binding energy surface, and they attributed the Pt catalyst detachment and agglomeration to the weak interaction between the Pt and the carbon support.[16] Experimental evidence also substantiates the link between the binding energy, dispersion degree and catalyst durability. For example, doping carbon nanotubes[17-19] or graphene nanoplatelets[20-22] increases the binding energy and also causes an increase in Pt dispersion, a resistance to agglomeration of the Pt nanoparticles, and a less significant deterioration of the activity when compared with the pure carbon cases.

Therefore, to improve the durability of Pt/C, the key problems are increasing the dispersion of the Pt nanoparticles and the binding energy between the Pt and the carbon support. Compared with doped carbon supports, pure carbon materials with physically adsorbed Pt are easy to produce and have fewer impurities that form under the operational environment; thus, developing novel pure carbon supports with high surface area, good electrical conductivity, suitable porosity to allow for a good reactant flux, and high stability in the fuel cell environment is a challenge that must be addressed.[9] Highly ordered CNT structures, such as well-aligned carbon nanotubes

(WACNTs), have special advantages over randomly oriented CNT cases, such as the ability to disperse Pt particles, electrochemical stability, and large surface area.[23-26] In addition, the trenches of the WACNTs may not only increase the binding energy between but also improve the utilization of Pt particles. For example, Tian et al. used vertically aligned carbon nanotubes as Pt support to prepare membrane electrode assembly (MEA), they found that the PEM fuel cell with the MEA showed an excellent performance with ultra-low Pt loading down to 35 μg cm^{-2} which was comparable to that of the commercial Pt catalyst on carbon powder with 400 μg cm^{-2}.[27] As a result, such WACNT structures are considered very promising electrode materials.

A molecular-level understanding of the mechanisms of the catalyst durability is required to identify the next generation of PEM fuel cell materials that have improved performance and prolonged operating life. Some simulation methods at the atomic or molecular scale have been implemented, such as density functional theories[28, 29] and molecular dynamics (MD) simulations.[30-33] Among the methods, classic molecular dynamics is a unique simulation method to explore the details of atomic processes at surfaces, especially those diffusion and aggregation processes encountered at the support-material surface.[34] Morrow et al. investigated the mobility and morphology of one Pt nanoparticle supported on WACNT and one-layer graphite through employing MD simulation; the results showed that Pt cluster with 249 atoms diffused at a lower rate when deposited on WACNTs than on graphite, and the lowest diffusion coefficient occurred on WACNT substrate.[35] However, the used models of one Pt cluster and one-layer graphite have a certain distance away from the experimental environments when they are considered as the catalyst of PEM fuel cells, where many Pt particles are deposited on the substrates and graphene may have a few layers as the substrate.[36] Besides, the trenches of the WACNTs adds the roughness degree of the substrate surface, which may decrease the aggregation probability of Pt clusters comparing with graphene substrate. Therefore, the dynamic process of Pt particles deposited on WACNT and graphene substrates still deserve to investigate.

In this work, we first establish the molecular models of WACNTs and Pt clusters

according to their corresponding experimental samples, and a four-layer graphene based on considering the vdW forces between Pt clusters and layers; then discuss the diffusion mechanism of Pt particles on the two support materials of WACNT and graphene, including a determination of the largest binding energy, diffusion coefficients and Pt loading without any agglomeration. This work aims to acquire the diffusion mechanism of Pt nanoparticles and determine the advantages of using WACNTs as support materials via MD simulations.

2. Simulation details

2.1 Model establishment

Before establishing a molecular model of Pt clusters, we use transmission electron microscopy (TEM) to investigate the morphology of Pt/carbon black (Hispec 3000) used as the catalyst of a PEM fuel cell, which was purchased from the Johnson Matthey (JM) Company. It can be seen from Fig. 1a that the Pt particles are dispersed evenly onto the surface of carbon black; the particles are spherical and are approximately 2 to 3 nm in size. Next, based on the bulk Pt crystal with an fcc structure and the corresponding lattice parameters (a = 0.392 nm and $\alpha = \beta = \gamma = 90°$) and the space group of Fm-3m, we established the Pt cluster with a size of 2.4 nm and with 556 atoms, which exhibit a shape that is truncated from a hexahedral shape, as shown in Fig. 1b. In addition, to investigate the size effect on the aggregation of Pt clusters, we also consider the model of a Pt cluster with a size of 1.2 nm and 80 atoms, as shown in Fig. 1c, which were obtained from the Cambridge Cluster Database[37].

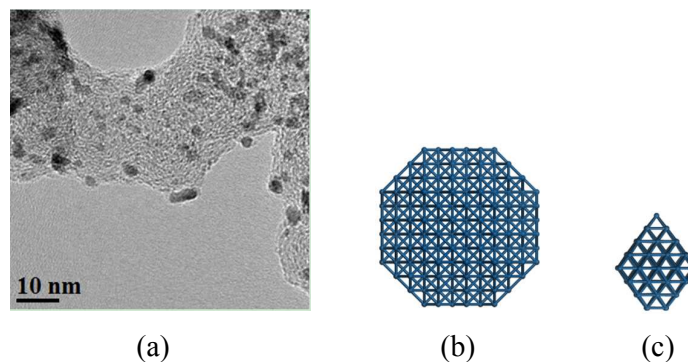(a)   (b)   (c)

Fig. 1 (a) the TEM picture of Pt/carbon black; (b) Pt cluster with a size of 2.4 nm; (c) Pt cluster with a size of 1.2 nm.
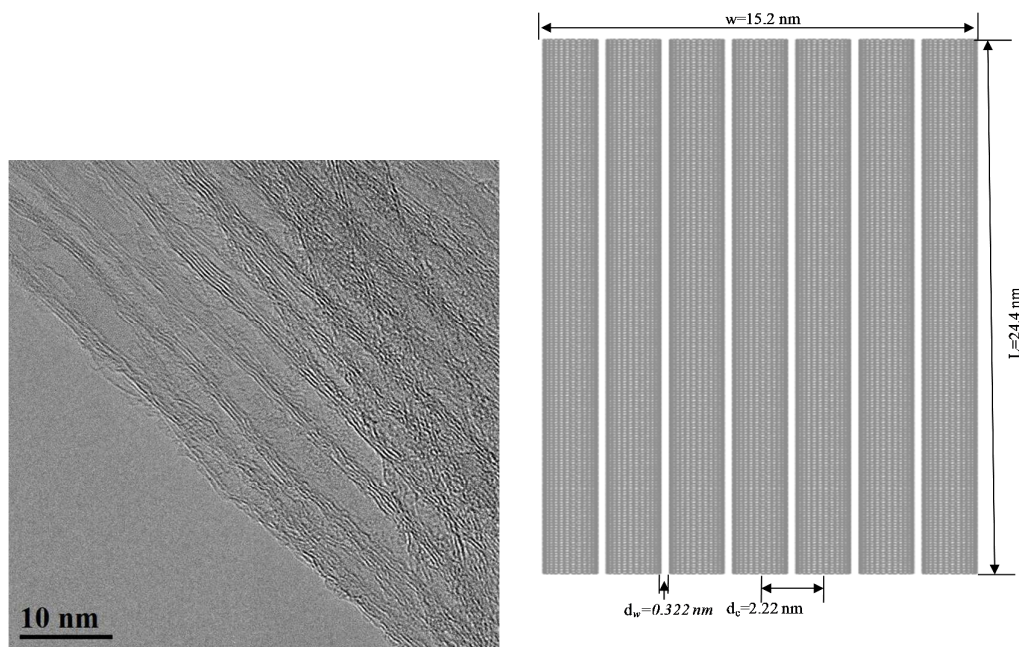

Fig. 2 (a) The TEM picture of WACNT; (b) sketch of WACNT (14, 14) with a length of 24.4 nm and a width of 15.2 nm.

The morphology of WACNT is also investigated, as shown in Fig.2a that is a TEM picture of WACNT sample (supplied by Jiedi Nanotechnology Company). It is seen that multi-walled CNTs, with the similar diameters of 5 nm around, are well aligned. In this work, we mainly consider WACNT models composed of armchair single-walled CNTs (SWCNTs) with various tube diameters. Those are in an arrangement with uniform spacing between the SWCNTs. Given an example of WACNT (14, 14), as depicted in Fig. 2b, it has a vertical length (L) of 24.4 nm and a distance (d_c) of 2.22 nm between two central points of two neighbouring SWCNTs in the same horizontal direction; thus, the spacing distance between two adjacent walls (d_w) along the centre line is 0.322 nm, i.e., the distance of dc minus the diameter (d) of a SWCNT (14, 14). After establishing the WACNT model, the Pt clusters will be

randomly and evenly dispersed onto the surface of the WACNTs, and the close

contact will be monitored, where the distance away from selected atomic radii of less

than 0.891 Å is considered to be the point at which the van der Waals (vdW)

interaction occurs between Pt clusters and its substrate; a pink dashed line is used to

indicate such a close contact in the Materials Studio software. The Pt clusters will be

set well above the surface of the WACNTs when the pink line is just beginning to

appear. In this research, to determine the largest binding energy between Pt clusters

and the WACNT substrate, various geometric parameters of the WACNTs are

considered, along with various numbers of walls for each individual CNT.

2.2 Simulation method

Geometrical optimisation should first be performed on the initially constructed

Pt/WACNT configurations, where the bottom of the WACNTs is constrained. A

universal force-field (UFF), [38] embedded in Materials Studio software, is used to

describe the interaction of all atoms, including the interaction of the platinum atoms

and the carbon atoms. The functional form of UFF includes a harmonic valence term,

a three-term cosine-Fourier expansion for angle bending and additional cosine-Fourier

expansion terms for torsions and inversions. UFF has been widely used[39] and tested in

the similar systems containing all the atoms of which the models used in the present

work. [40, 41]

Next, a 30-ps dynamics simulation, with a time step of 0.5 fs and an NVT

(constant temperature and volume) ensemble, is first performed for the Pt/WACNT

molecular system to enable the initial temperature to quickly converge to the object

value (300 K) using the Berendsen thermostat method.[42] Subsequently, a quench

dynamics simulation, with a 100-ps simulation time and time step of 0.5 fs, is used to

find the equilibrium structure with the lowest energy. A Nose thermostat [43] is used to

control the temperature of the dynamics in this simulation process. Consecutively,

using the final equilibrium structure in the above simulation as the initial

configuration of the subsequent quench dynamics simulation, we will study the

diffusion process of the Pt clusters on the substrates, including the absorption location,

the binding energy, the diffusion coefficient and the aggregation probability of Pt clusters. In the second quench dynamics simulation, a time step of 2 fs and a simulation time of 900 ps are exploited, and the Nose method is also used here. Thus, simulations with a total simulation time of approximately 1 ns are performed. The cut-off distances of the vdW force are all set to 12.5 Å in the simulations. Additionally, the binding energy is calculated from the total energy of the ACNT-Pt minus the sum of the energies of the WACNTs and the Pt clusters.

The quench molecular dynamics simulations used here aim to find the equilibrium states with many local optimisations and a global optimisation during the total simulation time. Next, the diffusion mechanism of Pt clusters on their substrates is studied by calculating the dynamic trajectories, binding energy, diffusion coefficient, and Pt loading.

2.3 Diffusion coefficient

For a system at equilibrium, the particles will move in accordance with the equations of motion that define the system and, in general, will tend to diffuse away from their original location. The mean square displacement (MSD) of the particles with respect to their original position is obtained as the second moment of their distribution at $t > 0$, which is related to the diffusion coefficient (D) as follows:

$$D = \frac{1}{6}\frac{1}{N}\lim_{t \to \infty}\frac{d}{dt}\sum_{i=1}^{N} < [r_i(t) - r_i(0)]^2 > \tag{1}$$

where N is the number of Pt particles, $r_i(t)$ is the position of Pt i at time t, and the angular bracket ($< >$) denotes an ensemble average. In order to balance the computational time and the accuracy of the simulation results, the max simulation time of 1 ns is used and it is qualified for analyzing the binding energy and the trend of the atomistic diffusion process. At the meanwhile, D is calculated through the relationship between the mean square displacement and the appropriate time.

2.4 Pt loading calculation

We roughly estimate the maximum amount of Pt clusters without aggregation for

Pt particles over the total simulation time. Furthermore, the Pt loading (L_{Pt}) is calculated according to the maximum Pt amount and the substrate area, as shown in the following formula:

$$L_{Pt} = \frac{\text{Mass of Pt atoms}}{\text{Area of substrate}} \qquad (2)$$

$$\text{Mass of Pt atoms} = \frac{\text{Number of Pt atoms} \times \text{Relative mass of Pt atom}}{1.667 \times 10^{27}} \text{kg} \qquad (3)$$

Here, the relative mass of the Pt atom is 195.1 according to the international atomic weight table.

3. Results

3.1 The adsorption energy

We first investigate the binding energies of individual Pt clusters, one with a diameter of 1.2 nm and the other with a diameter of 2.4 nm, on the substrates of WACNTs and graphene; here, each of the different WACNT substrates has seven individual CNTs, but with different geometric parameters, such as d, d_c, and d_w. We use quench dynamics simulations of simulation time of 100 ps and at a time step of 0.5 fs, to find the equilibrium structures with the largest binding energies for all of the Pt/WACNT configurations considered. In the quench process of each model, we record and save the equilibrium structures, including the velocities every 10000 steps; as a result, 21 Pt/WACNT structures are obtained. Next, the corresponding binding energies of these structures are calculated, and the largest energy is used as the adsorption energy. Table 1 lists the adsorption energy of one Pt cluster on each of the substrates of well-aligned SWCNTs considered, a well-aligned double-walled CNT (10, 10)-(5, 5), and a four-layer graphene substrate. From the results for the WACNTs (8, 8) with three different spacing distances (d_w), when the Pt cluster has 80 atoms and a diameter of 1.2 nm, the minimum and maximum binding energies were found at a d_w of 0.422 nm and 0.6 nm, respectively. Therefore, the distance of d_w is related to the adsorption energy. From the results for WACNTs (18, 18) and a Pt cluster with a diameter of 2.4 nm, as presented in Table 1, when d_w is 1.259 nm, the interaction force

between the Pt cluster and the WACNTs is the largest, which corresponds to the largest adsorption energy of -43.44 kcal/mol comparing with the other cases. The Pt clusters located in the trenches of parallel aligned CNTs has the largest binding energy: in this case, the Pt cluster can experience the vdW interaction forces from two CNTs (see Fig. 3).
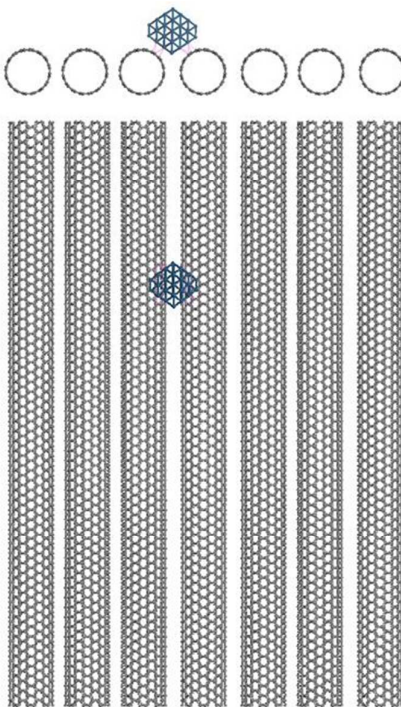

Fig. 3 Sketch of WACNTs (8, 8) with a d_w of 0.322 nm, which has the largest binding energy determined during the 100 ps quench time. The pink dotted line in the figure indicates the close contact between the C and Pt atoms.

Table 1 - The largest binding energy between one Pt cluster and its substrate and the corresponding parameters.

WACNTs	d(nm)	d_w (nm)	d_c(nm)	d_{Pt}(nm)	E_b(kcal/mol)
(5,5)	0.678	0.322	1	1.2	-20.88
(7,7)	0.949	0.322	1.27	1.2	-23.34
(8,8)	1.085	0.322	1.41		-24.68
		0.422	1.51	1.2	-26.52
		0.6	1.69		-16.2
(10,10)	1.356	0.322	1.68	1.2	-26.9
		0.5	1.86	1.2	-16
		0.322	1.68	2.4	-36.42
(10,10)-(5,5)	1.356	0.322	1.68	1.2	-27.46
(12,12)	1.627	0.322	1.95	1.2	-27.44
		0.422	2.05	1.2	-26.4
		0.322	1.95	2.4	-37.68
(14,14)	1.898	0.322	2.22	1.2	-27.69
		0.322	2.22	2.4	-39.14
		0.422	2.32	2.4	-34.04
(15,15)	2.034	0.322	2.36	1.2	-27.1
		0.322	2.36	2.4	-38.58
		0.659	2.69	2.4	-34.45
(16,16)	2.17	0.322	2.49	2.4	-39.1
(18,18)	2.441	0.322	2.76		-33.2
		0.659	3.1		-36.6
		0.859	3.3		-41.5
		1.059	3.5	2.4	-42.2
		1.259	3.7		-43.44
		1.459	3.9		-41.07
(24,24)	3.254	1.259	4.51	2.4	-45.03
(28,28)	3.797	1.259	5.06	2.4	-43.92
(30,30)	4.068	1.259	5.33	2.4	-43.9
Graphene (four layer)				1.2	-20.9
				2.4	-35.04

Except for the distance of d_w, the diameter of the SWCNT also has an important influence on the binding energy. As indicated in Table 1, when the size of the Pt cluster and the spacing distance are set, the adsorption energy will first increase with the CNT diameter (also the depth of the WACNTs), followed by saturation to a constant value (or have a very slight fluctuation). For example, when d_w is 0.322 nm and d_{Pt} is 1.2 nm, the binding energy will increase with the CNT diameter up to

approximately 1.9 nm, i.e., WACNTs (14, 14), and then with the increase in the CNT diameter, the adsorption energy will exhibit a slight decrease; this situation can also be observed when d_w is 1.259 nm and d_{Pt} is 2.4 nm, in which case WACNTs (24, 24) with a d of 3.254 nm will supply the largest adsorption force. This largest adsorption force is mainly caused by the increase of the trench area: it is known that an increase in the CNT diameter will also lead to an increase in the trench area if the spacing distance is a constant, i.e., the vdW interaction area between WACNTs and Pt cluster will begin to augment, and then the vdW force and the binding energy also become stronger until they both have an adequate interaction; in this case, a continuous increase in the CNT diameter will not cause the binding energy to further increase. Note that the diameter of Pt cluster (1.2 nm) is larger than the spacing distance (0.322 nm).

Furthermore, we investigated the adsorption behaviour of one Pt cluster on the graphene substrate with different numbers of layers, such as three, four, six and eight layers. However, due to the setting values of 12.5 Å for the cut-off distances of the vdW force and the distance of 3.4 Å between two adjacent graphene layers in our simulations, the results did not indicate much change when the number of layers is larger than four, and the first three layers exhibit a more obvious vdW interaction with the adsorbed Pt cluster, that is to say, fewer or zero vdW interaction force exists between the Pt clusters (above the first layer) and the layers whose number are larger than four. Therefore, in the next work, four–layer graphene will be used as the substrate for investigating the adsorption and diffusion behaviour of Pt clusters, with the carbon atoms in the last layer away from Pt cluster being constrained. The data in Table 1 indicate that the adsorption energies of Pt clusters on graphene are obviously smaller than those on WACNTs (and more obviously smaller than those on WACNTs with larger CNT diameters). These results demonstrate that there are stronger vdW force interactions between WACNTs and Pt clusters than there are between graphene and the Pt clusters.

In addition, we investigated the influence of the number of walls of CNTs, for example, a double-walled CNT (10, 10)-(5, 5) is considered to construct the WACNTs.

Compared with SWCNT (10, 10), double-walled CNT can provide a greater vdW force to the Pt cluster, yet the increase in the vdW force is not more obvious than that from the influence of the CNT diameter. Thus, in the next work, we mainly considered WACNT models composed of SWCNTs.

3.2 The diffusion mechanism

For a given Pt cluster, based on the equilibrium structure with the largest adsorption energy in Table 1, we constructed molecular models of Pt/WACNTs with multiple Pt clusters and then investigated their diffusion mechanism, i.e., WACNTs (14, 14) with a d_w of 0.322 nm and WACNTs (24, 24) with a d_w of 1.259 nm are used for supporting a Pt cluster with a diameter of 1.2 nm and a Pt cluster with a diameter of 2.4 nm. In addition, the diffusion mechanics of these two types of Pt clusters on a graphene substrate is also considered by using the same quench dynamics simulation. The diffusion mechanism mainly includes the largest binding energy, diffusion coefficient, aggregation probability and Pt loading.

3.2.1 The equilibrium structures and the corresponding binding energy

In order to examine the aggregation and dispersion characteristics of Pt clusters on the substrate, we need to first analyze the equilibrium structures of Pt/substrate at different simulation times, and then calculate the binding energies of Pt cluster - substrate and Pt cluster - Pt cluster to study the structural stability. When WACNTs (14, 14) and graphene have a similar bottom area of 372 nm^2, 36 Pt clusters with the same diameter of 1.2 nm are considered to investigate their diffusion behaviour. Pt clusters are evenly laid onto the substrates in the initial configurations, as shown in Figs. 4a$_1$ and 4b$_1$. Next, MD simulations are conducted, and the equilibrium structures at the dynamic times of 100 ps and 1 ns for WACNTs are shown in Figs. 4a$_2$ and 4a$_3$, respectively, and the equilibrium structures at the dynamic times of 100 ps and 1 ns for graphene are shown in 4b$_2$ and 4b$_3$, respectively. From the structures at 100 ps (Figs. 4a$_2$ and 4b$_2$), the Pt clusters are distributed much more evenly on the surface of the WACNTs than on the surface of graphene, except that two pairs of Pt clusters tend to be aggregated on the surfaces of both WACNTs and graphene, as indicated by the

red dashed-line circles in Fig. 4. When the simulation time continues up to 1 ns, the aggregation of Pt clusters on the graphene surface becomes much more obvious than that on the WACNT substrate surface, and the distribution structure (Fig. $4b_3$) indicates that there is still an increasing trend for the aggregation of Pt clusters with the increasing simulation time.

Furthermore, we characterise the aggregation degree of Pt clusters (indicated by red circles in Figs. $4a_3$ and $4b_3$) by calculating the binding energy, as listed in Table 2. The binding energies of the Pt clusters on the WACNT substrate surface are generally smaller than those on the graphite surface, i.e., the binding strength and aggregation degree of the Pt clusters on the graphene substrate are greater than those on the WACNT substrate. Here the binding strength and aggregation degree are closely related with the binding energy. The larger the binding energy of Pt clusters is, the greater their binding strength (or vdW force) will be, so Pt clusters will be easily aggregated, i.e., their aggregation degree or probability will become large. The aggregated Pt clusters with a small interaction force will be detached at the longer simulation time, while for the cases with great interaction force, the clusters are unlikely to become detached from each other at the longer simulation time. For example, the two Pt clusters of Pair 6 on graphene surface, with the binding energy of -2.14 kcal/mol (see Table 2), are hard to detach from each other even at a very long simulation time compared with any Pairs on WACNT surface. Therefore, Pt particles with a diameter of 1.2 nm are easier to suffer from agglomeration on the graphene surface than on the WACNT surface.

In addition, the binding stability of the Pt clusters and their substrates are also investigated based on the adsorption energies, i.e., the largest binding energy in the total simulation process. For the substrate, the adsorption energies of Pt clusters on WACNTs and graphene substrates are -893 kcal/mol and -638 kcal/mol, respectively; this result demonstrated that the equilibrium structure of Pt/WACNTs is more stable than that of Pt/graphene. And the magnitude of 1 kcal/mol for the binding energy of the pairs of Pt clusters is far less than that of average binding energy between one Pt cluster and substrate, i.e., 24.8 kcal/mol for WACNT substrate and 17.7 kcal/mol for

graphene substrate. It illustrates that the binding stability between Pt cluster and its substrate is much better than that between Pt clusters.
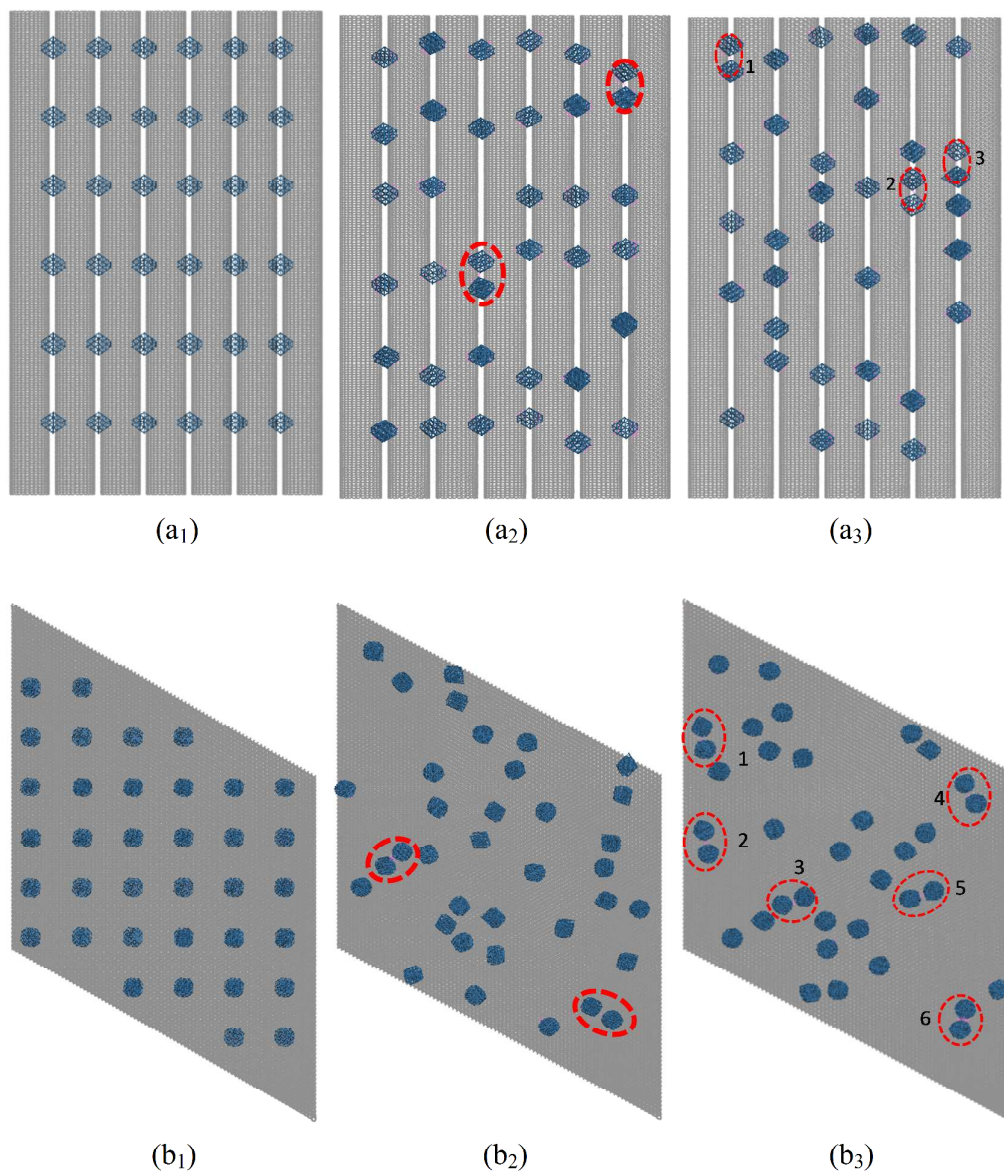
Fig. 4 (a_1) The initial configuration of 36 Pt clusters on the WACNT (14, 14) substrate surface with 100 units for each CNT and a wall distance (d_w) of 0.322 nm; (a_2) the equilibrium structure for (a_1) at a dynamic time of 100 ps; (a_3) the equilibrium structure for (a_1) at a dynamic time of 1 ns. (b_1) The initial configuration of 36 Pt clusters on the graphene surface that have the same bottom area as the WACNT substrate surface; (b_2) the equilibrium structure for (b_1) at a dynamic time of 100 ps; (b_3) the equilibrium structure for (b_1) at a dynamic time of 1 ns. The red circles indicate the aggregation probability of the Pt clusters.

Table 2 - The binding energy of the pairs of Pt clusters in Fig. 4.

Types	binding energy (kcal/mol)
WACNTs Pair 1	-0.74
WACNTs Pair 2	-0.59
WACNTs Pair 3	-0.71
graphene Pair 1	-0.88
graphene Pair 2	-0.52
graphene Pair 3	-0.87
graphene Pair 4	-0.77
graphene Pair 5	-0.74
graphene Pair 6	-2.14

Subsequently, Pt clusters with a diameter of 2.4 nm were also studied based on the substrates of WACNT (24, 24) and graphene, with both having the same bottom area of approximately 895 nm^2. In the initial configuration of Pt/WACNTs (24, 24), four Pt clusters are evenly laid in each trench of the WACNTs, where the length of each individual CNT is 29.5 nm, and the wall distance (d_w) is 1.259 nm. Based on the equilibrium structures at the 100 ps dynamic time (Figs. 5a_1 and 5b_1), no aggregation trend for Pt clusters was found, either on the WACNT substrate surface or on the graphene surface. After a continuous dynamic simulation time of approximately 900 ps, the equilibrium structures indicated that more Pt clusters trend to be aggregated on the graphene surface than on the WACNT surface, as indicated by the red dashed line in Figs. 5a_2 and 5b_2.

Moreover, the calculated adsorption energies of the Pt clusters on WACNT (24, 24) and graphene substrates were found to have values of -1063 kcal/mol and -843 kcal/mol, respectively. The corresponding average binding energy between one Pt cluster and substrates are -44.3 kcal/mol for WACNT substrate and -35.1 kcal/mol for graphene substrate. And it is also illustrated that the average binding energies for the Pt clusters of diameter of 2.4 nm are larger than those of the Pt clusters of diameter of 1.2 nm. Therefore, based on the binding energy, the 24-Pt / WACNTs (24, 24) structure is more stable than the other three models, i.e., the 24-Pt / graphene, 36-Pt / WACNTs (14, 14), and 36-Pt / graphene models.
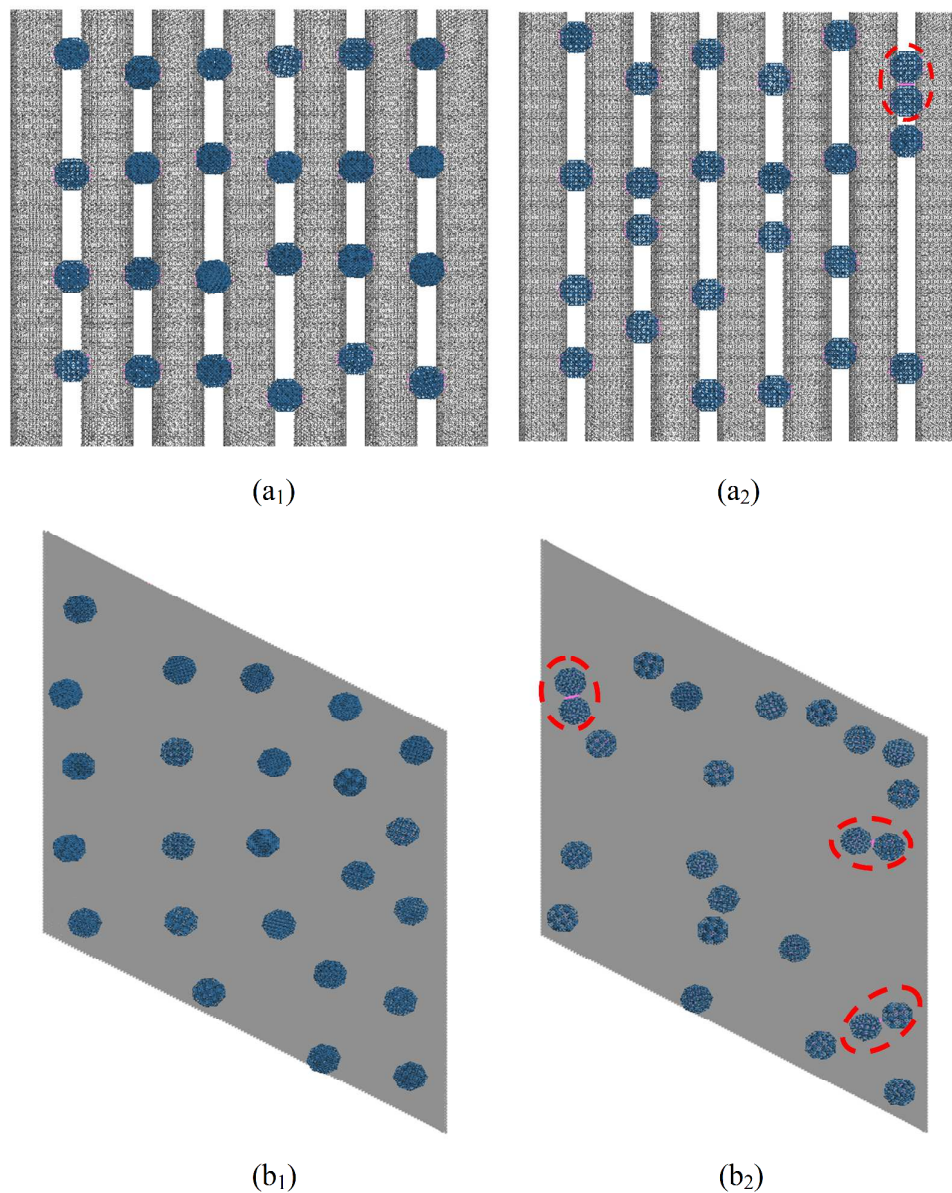
Fig. 5 The equilibrium structure of the 24-Pt / WACNTs (24, 24) structure (a_1) at a dynamic time of 100 ps and (a_2) at a dynamic time of 1 ns; the equilibrium structure of 24-Pt / graphene structure (b_1) at a dynamic time of 100 ps and (b_2) at a dynamic time of 1 ns. The two substrates have similar values of the bottom area. The pink connection lines between the aggregated Pt clusters, as highlighted by the red circles, indicate the interactions of the vdW force.

3.2.2 Diffusion coefficient

The relationship between the mean square displacement and the dynamic time is

collected for Pt/substrates. In addition, the diffusion coefficients are analysed from 0 to 480 ps, as presented in Fig. 6 and Table 3. As expected, the slope of the curves increases with the decrease of the size of Pt clusters when their substrates are of the same type, and it is clear that the slopes of the curves for Pt clusters on the graphene surface are larger than those for Pt clusters on the WACNT substrate surface. According to Eq. (1), the slope of curve is proportional to the diffusion coefficient. Therefore, as indicated in Table 3, the Pt clusters, with the same sizes and shapes, on the graphene substrate exhibit a larger value of D than those on the WACNT substrate surface; in addition, for each type of substrate, the diffusion coefficient decreases with the increase of the size of the Pt cluster. The calculated diffusion coefficients, ranging from 0.8×10^{-5} cm^{2}s^{-1} to 8.8×10^{-5} cm^{2}s^{-1}, are similar as that of previous work at the temperature of 300 K; [35, 44] and they affected not only by the support materials but also by the size of Pt particles.
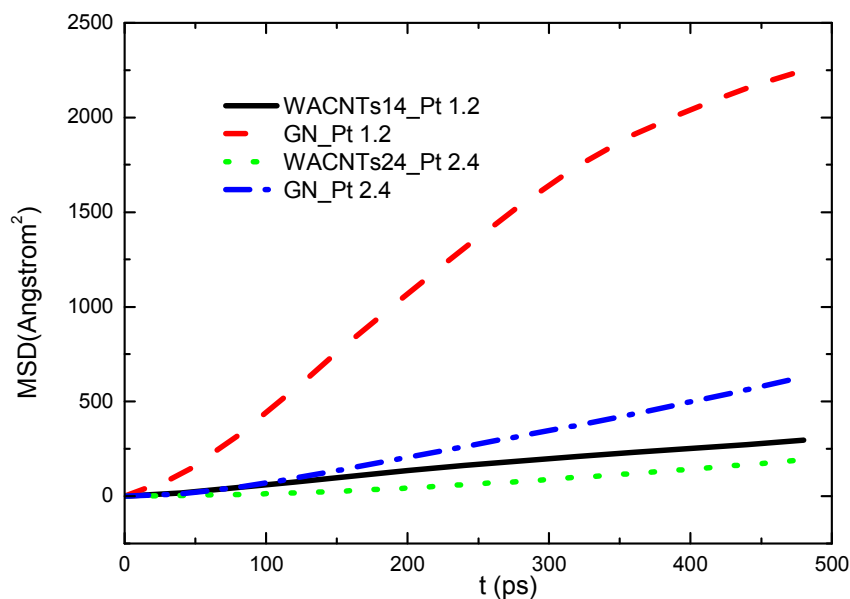

Fig. 6 The relationship between MSD and time for Pt clusters with diameters of 1.2 nm and 2.4 nm on the substrates of WACNTs and graphene.

Table 3 The diffusion coefficients of the Pt clusters on their substrates.

Model	WACNTs14_Pt1.2	GN_Pt1.2	WACNTs24_Pt2.4	GN_Pt2.4
$D(cm^2s^{-1})$	1×10^{-5}	8.8×10^{-5}	0.8×10^{-5}	2.4×10^{-5}

Note: graphene is denoted by GN in Tab.3.

It is known that the larger the diffusion coefficient is, the easier the aggregation of Pt clusters will be. This result agrees well with the conclusion of the final equilibrium structures and the binding energy presented in section 3.2.1, i.e., the aggregation probability of the Pt clusters on graphene is larger than that on WACNTs, and the Pt cluster with a diameter of 2.4 nm is less easily aggregated than the Pt cluster with a diameter of 1.2 nm. This evidence indicates that there are close links among the binding energy, the diffusion coefficient, and the aggregation degree.

3.3 Pt loading

According our simulation results for various models, we infer the maximum number of Pt clusters without any agglomeration for a substrate with a given bottom area. Because WACNTs can support greater amounts of Pt clusters than graphene, the Pt loading based on WACNT substrates are only calculated according to Eq. (2). When the substrate is composed of WACNTs (14, 14) with a bottom area of 372 nm^2 and each Pt cluster has 80 Pt atoms (see Fig. 4a$_3$), in the supported 36 number of Pt clusters, three pairs of Pt clusters are aggregated; however, the interaction forces between the pairs are very small (as indicated in Table 2). Therefore, we suppose that if a Pt cluster on each aggregated pair is removed, there will be a reduced aggregation probability, or even the lack of occurrence of aggregation. Next, we estimate that the maximum amount of 33 Pt$_{80}$ clusters can be supported on this WACNT substrate surface; thus, according to Eqs. (2) and (3), the Pt loading (L_{Pt}) is 0.083 μg/cm^2. Additionally, when the substrate is WACNTs (24, 24) with a bottom area of 892 nm^2 and each Pt cluster has 556 Pt atoms, only two Pt clusters are aggregated at a dynamic time of 1 ns, as shown in Fig. 5a$_2$; thus, we infer that the maximum loading amount of Pt clusters is 23 on this substrate, which corresponds to a value of L_{Pt} of 0.167 μg/cm^2.

The substrate of WACNTs (24, 24) were found to support a larger Pt loading, although the amount of Pt clusters is smaller and the substrate area is larger than that of the substrate of WACNTs (14, 14). Thus, Pt loading is more closely related with both the sizes of the Pt clusters and the WACNTs and the binding energy. In addition, the Pt loading may also be affected by the shape of Pt cluster. In this work, the shape of the Pt cluster of diameter of 2.4 nm is spherical, and the shape of the Pt cluster of diameter of 1.2 nm is conical. Similar to the catalyst purchased from the JM Company (see Fig. 1a), the shapes of the Pt particles are primarily spherical or round from the two-dimensional perspective.

4. Discussion

Due to the existence of the trenches in the WACNT substrates, the binding force between the Pt clusters and WACNTs is much larger than that between the Pt clusters and graphene. This behaviour not only decreases the aggregation probability of the Pt clusters but also increases their binding stability. Moreover, if the number of walls of each individual CNT increases, the binding vdW force between the Pt clusters and the WACNT substrate will be comparable to that of chemical adsorption, which will add new chemical elements to pollute the cell system.

Although Pt loading is reported on the order of 35 μg cm^{-2},[27] in the near future, if we can control the molecular arrangement on the substrate, the maximum amount of Pt clusters may be realized for a given WACNT substrate. As the catalyst of PEMFCs, the maximal Pt loading may be as a reference for decreasing the aggregation probability, certainly the catalytic efficiency should be firstly ensured.

5. Conclusions

Well-aligned carbon nanotubes for use as Pt support materials were studied using MD simulations. By investigating various Pt/WACNTs models, it is found that the trenches in WACNTs correspond to the best adsorption locations and can supply a larger binding energy than the other locations. The binding energy is determined by the sizes and shapes of the Pt clusters and the geometrical parameters of the WACNTs

of CNT diameter, spacing distance and wall-number of the CNT, especially the CNT diameter. Note that the largest binding energy is obtained at the ratio of Pt-particle diameter to CNT diameter in the range from 0.6 to 0.7.

For the same substrate area of WACNTs and graphene, we studied the diffusion process of the Pt clusters by observing the equilibrium structures and calculating the binding energy, diffusion coefficient and Pt loading. Compared with the graphene substrate, the use of a WACNT substrate can decrease the aggregation probability while increasing the binding stability and Pt loading, thus, it is a promising support material of Pt particles in the application of the catalyst of a PEM fuel cell.

Acknowledgements

References

[1] D. A. Stevens, and J. R. Dahn, *Carbon*, 2005, **43**, 179-188.

[2] J. Xie, D. L. Wood III, D. M. Wayne, T. A. Zawodzinski, P. Atanassov, and R. L. Borup, *J. Electrochem. Soc.*, 2005, **152**, A104-A113.

[3] S. D. Knights, K. M. Colbow, J. St-Pierre, and D. P. Wilkinson, *J. Power Sources*, 2004, **127**, 127–134.

[4] K. C. Lee, J. J. Zhang, H. J. Wang, and D. P. Wilkinson, *J. Appl. Electrochem.*, 2006, **36**, 507−522.

[5] W. M. Zhang, P. Sherrell, A. I. Minett, J. M. Razal, and J. Chen, *Energ. Environ. Sci.*, 2010, **3**, 1286–1293.

[6] E. Antolini, *Appl. Catal. B*, 2009, **88**, 1-24.

[7] B. Serger, and P. V. Kamat, *J. Phys. Chem. C*, 2009, **19**, 7990-7995.

[8] Y. G. Li, W. Gao, L. J. Ci, C. M. Wang, and P. M. Ajayan, *Carbon*, 2010, 48: 1124-1130.

[9] P. J. Ferreira, G. J. La O', Y. Shao-Horn, D. Morgan, R. Makharia, S. Kocha, and H. A. Gasteiger, *J. Electrochem. Soc.*, 2005, **152**, A2256-A2271.

[10] F. Maillard, S. Schreier, M. Hanzlik, E. R. Savinova, S. Weinkauf and U. Stimming, *Phys. Chem. Chem. Phys.*, 2005, **7**, 385-393.

[11] Y. Y. Shao, G. P. Yin, and Y. Z. Gao, *J. Power Sources*, 2007, **171**, 558−566.

[12] X. Yu, and S. Y. Ye, *J. Power Sources*, 2007, **172**: 145−154.

[13] W. Bi, T. F. Fuller, *J. Power Sources*, 2008, **178**, 188-196.

[14] S. Ban, K. Malek, C. Huang, *J. Power Sources*, 2013, **221**, 21-27.

[15] H. Yano, J. Inukai, H. Uchida, M. Watanabe, P. K. Babu, T. Kobayashi, J. H. Chung, E. Oldfield and A. Wieckowski, *Phys. Chem. Chem. Phys.*, 2006, **8**, 4932-4939.

[16] M. N. Groves, C. Malardier-Jugroot, and M. Jugroot, *J. Phys. Chem. C*, 2012, **116**, 10548-10556.

[17] Y. G. Chen, J. J. Wang, H. Liu , R. Y. Li, X. L. Sun, S. Y. Ye, and S. Knights, *Electrochem. Commun.*, 2009, **11**, 2071-2076.

[18] H. Feng, J. Ma, and Z. Hu, *J. Mater. Chem.*, 2010, **20**, 1702−1708.

[19] W. An, and C. H. Turner, *J. Phys. Chem. C*, 2009, **113**, 7069−7078.

[20] R. I. Jafri, N. Rajalakshmi, and S. Ramaprabhu, *J. Mater. Chem.*, 2010, **20**, 7114-7117.

[21] T. Holme, Y. Zhou, R. Pasquarelli, and R. O'Hayre, *Phys. Chem. Chem. Phys.*, 2010, **12**, 9461−9468.

[22] C. K. Acharya, D. I. Sullivan, and C. H. Turner, *J. Phys. Chem. C*, 2008, **112**, 13607−13622.

[23] H. Tang, J. H. Chen, Z. P. Huang, D. Z. Wang, Z. F. Ren, L. H. Nie, Y. F. Kuang, and S. Z. Yao, *Carbon*, 2004, **42**,191-197.

[24] Y. Liu, J. Chen, W. M. Zhang, Z. F. Ma, G. F. Swiegers, C. O. Too, and G. G. Wallace, Chem. Mater., 2008, **20**, 2603-2605.

[25] Y. Yuan, J. Smith, G. Goenaga, D. J. Liu, B. Zhou, and J. B. Liu, *J. Exp. Nanosci.*, 2013, **8(6)**, 797−807.

[26] R. B. Wu, B. S. Li, K. Zhou, S. H. Chan, J. N. Tey, J. Wei, L. Li, X. Wang, and L. Y. Wang, Chem. Eur. J., 2013, **19**, 9155-9159.

[27] Z. Q. Tian, S. H. Lim, C. K. Poh, Z. Tang, Z. Xia, Z. Luo, P. K. Shen, D. Chua, Y. P. Feng, Z. Shen, and J. Lin, *Adv. Eng. Mater.*, 2011, **1**, 1205-1214.

[28] S. Alayoglu, A. U. Nilekar, M. Mavrikakis, and B. Eichhorn, Nat. Mater., 2008, **7**, 333-338.

[29] J. R. Kitchin, J. K. Nørskov, M. A. Barteau, and J. G. Chen, J. Chem. Phys., 2004, **120**, 10240-10246.

[30] P. Braulta, A. Caillard, C. Charles, R. W. Boswell, and D. B. Graves, *Appl. Surf. Sci.*, 2012, **263**, 352-356.

[31] D. H. Seo, H. Y. Kim, J. H. Ryu, and H. M. Lee, *J. Phys. Chem. C*, 2009, **113**, 10416−10421.

[32] M. C. Wu, C. L. Li, C. K. Hu, Y. C. Chang, Y. H. Liaw, L. W. Huang, C. S. Chang, T. T. Tsong, and T. Hsu, *Phys. Rev. B*, 2006, **74**, 125424-8.

[33] Q. P. He, D. C. Joy, and D. J. Keffer, *J. Power Sources*, 2013, **241**, 634-646.

[34] L. J. Lewis, P. Jensen, N. Combe, and J. L. Barrat, *Phys. Rev. B*, 2000, **61**, 16084-16090.

[35] B. H. Morrow, and A.Striolo, *J. Phys. Chem. C*, 2007, **111**, 17905-17913.

[36] S. M. Unni, V. K. Pillai, and S. Kurungot, *RSC Adv.*, 2013, **3**, 6913-6921.

[37] D. J. Wales, J. P. K. Doye, A. Dullweber, M. P. Hodges, F. Y. Naumkin, F. Calvo, J. Hernández-Rojas, and T. F. Middleton, *URL: http://www-wales.ch.cam.ac.uk/CCD.html*.

[38] A. K. Rappé, C. J. Casewit, K. S. Colwell, W. A. Goddard, and W. M. Skiff, *J. Am. Chem. Soc.*, 1992, **114**, 10024-35.

[39] J. H. Yuan, and K. M. Liew, *Phys. Chem. Chem. Phys.*, 2014, **16**, 88-94.

[40] J. Szczygiel, and B. Szyja, *J. Mol. Graphics Modell.*, 2006, **25**, 116–125.

[41] P. Fouquet, M. R. Johnson, H. Hedgel, A. P. Jardine, J. Ellis, W. Allison, *Carbon*, 2009, **47**, 2627-2639.

[42] H. J. C. Berendsen, J. P. M. Postma, W. F. van Gunsteren, A. DiNola, and J. R. Haak, *J. Chem. Phys.*, 1984, **81**, 3684-3690.

[43] S. Nosé, *Mol. Phys.*, 1984, **52**, 255-268.

[44] S. Chen, and A. Kucernak, *J. Phys. Chem. B*, 2003, **107**, 8392-8402.